Numerical investigation in coated carbide tool using *COMSOL* and inverse problems

DC Ferreira, ES Magalhães, RF Brito and SMM Lima e Silva*

Federal University of Itajuba - Heat Transfer Laboratory, Itajuba, MG, Brazil.

* metrevel@unifei.edu.br

Abstract. The determination of the thermal field in a turning process is important to improve the process quality. Recently, the carbide tools have been coating with ceramic materials that present insulating characteristics. This work presents the thermal effects of coatings in a carbide tool during a turning process using the *COMSOL* software and a non-linear inverse problem. The thermal model consists of a coated carbide tool, a tool holder and a shim described by the transient non-linear three-dimensional heat diffusion equation with heat loss by convection and radiation. The unknown heat source was obtained through the Specification Function Method. In order to validate the methodology, the heat input was compared with a previous work. Titanium nitride (TiN) and aluminium oxide (Al$_2$O$_3$) are utilized as the coating materials. Both coatings presented the expected behaviour when less heat is dissipated to the cutting tool substrate. The coated carbide tools presented higher maximum temperatures in the contact area than the uncoated carbide tool. The work also found that when the coating thickness increases the maximum temperature in the contact area also increases. The results presented in this works may help the development of new coated carbide tools with a higher lifespan.

1. Introduction

Reducing machining costs and the bad effects caused by using cooling lubricants are the main advantages of dry machining. However, to better understand the physical phenomena involved in this process, it is necessary to model it in the most realistic way [1,2]. It is difficult to determine the temperature on the tool-chip interface due to the movement of the workpiece, chip obstruction and the small tool-chip contact area.

Experimental methods have their limitation to determine this temperature. In embedded thermocouple method, the position of the thermocouple close to the tool-chip contact area can interfere in the heat flux. Infrared methods also have their limitation, once it is not possible to measure the temperature directly due to chip obstruction on the rake face. Lately, numerical methods, like finite element method and finite difference method, have also been applied to simulate the tool-chip interface temperature. Nevertheless, without precisely knowing the heat flux at tool-chip interface, these methods cannot determine the cutting temperature directly [3]. Thus, inverse heat conduction techniques represent a good alternative to obtain this temperature. These techniques allow the use of experimental data obtained from accessible regions [4].

A comparison of the inverse techniques Golden Section, Specification Function, Simulated Annealing and Dynamic Observers based on Green function was proposed by Carvalho *et al*. [5]. An experimental methodology used these techniques to determine the thermal fields and heat generated in

the tool-chip interface during turning process. Liang *et al*. [6] proposed a quantitative investigation of temperature at the tool-chip interface during a machining process using a heat pipe as a heat exchanger to cool a cutting tool. The finite difference method and an inverse procedure were used to determine the temperature. Similar work was also carried out by Liang *et al*. [3], which presented an inverse three-dimensional procedure to investigate the tool-chip interface temperature in dry turning of the AISI 1045 steel. Using an infrared thermography camera the temperature on the rake face of the cutting tool was measured and later used to obtain the heat flux by the conjugate gradient method.

Brito *et al*. [4] improved the work of [7] and [8] and proposed a more complex geometry to better represent the numerical model of the thermal problem in turning. The Specification Function and the commercial software *COMSOL* were used to estimate the heat flux and the temperature field at the contact area in a cutting tool. The inverse heat conduction method has also been applied in the study of other machining processes. The amount of energy transferred to the workpiece during electric discharge machining process (EDM) was estimated using the Lavenberg-Marquardt method [9]. Almost all the energy is lost through convection and radiation to the dielectric fluid and by conduction via the tool.

The *COMSOL* Multiphysics is FEA software (Finite Element Analysis) based on advanced numerical methods to model and solve physical problems. Gerlich *et al*. [10] presented a software validation for a calculation of heat transfer in buildings. The heat transfer calculation in the *COMSOL* Multiphysics was validated by the comparative verification provided by the International Energy Agency and by the comparison of the measured data in real building segment. Greiby *et al*. [11] used an ordinary least square and a sequential estimation method in MATLAB with *COMSOL* to sequentially estimate a temperature-dependent thermal conductivity of a cherry pomace. Suarez *et al*. [12] studied the heat transfer in solids using infrared photothermal radiometry and simulation using *COMSOL* Multiphysics. The good agreement between the results of numerical simulation and experimental data showed the potential of the software for the interpretation of photothermal experiments.

This work is an improvement of the work developed by Brito *et. al* [4]. The main difference consists of having non-linear convection and radiation in the *COMSOL* model. A new analysis of the maximum, minimum and average temperature in the contact area interface is presented. A numerical code in MATLAB in connection with *COMSOL* is used to calculate the heat flux. Once the heat flux is known, *COMSOL* is again used to solve the transient heat diffusion equation and obtain the temperature field in the model. The heat flux estimated in this work is compared with the heat flux of a previous work to validate the methodology. The differences of the maximum temperature in the contact area between the coated and uncoated carbide tool for different thickness coating values are also evaluated.

2. Methodology
2.1. The 3-D Models
The 3-D models consist of a coated and uncoated carbide tool, an AISI 1045 steel tool holder and a carbide shim. Figure 1 presents the fundamental dimensions of the models. These two numerical models are used in the simulation to compare the thermal effect of the coating on the thermal gradient created in the tool during the cutting process. This coating is present on the rake face of the cutting tool, where the workpiece and the cutting tool are in contact. A thin layer placed on the top surface of the substrate of the cutting tool represents the coating. The thermal contact between the coating and the substrate is considered perfect.
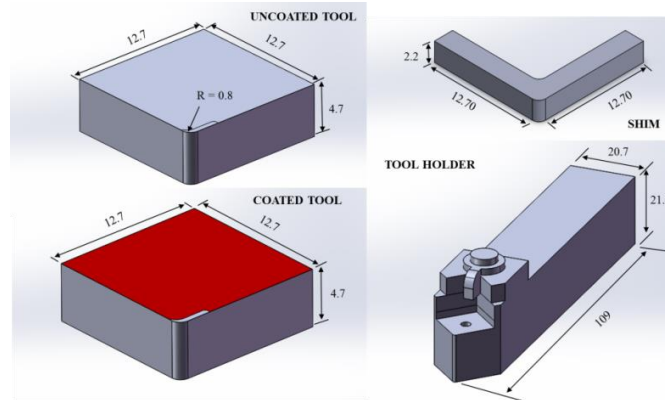
Figure 1. Fundamental dimensions of the 3-D models in mm.

To better exemplify, the models are divided into domains (Fig. 2): substrate of the carbide cutting tool (Ω_1), shim (Ω_2), tool holder (Ω_3) and coating (Ω_4). Subsequently, each domain is divided into regions submitted to different boundary conditions like imposed heat flux, convection, radiation and contact interface. Figure 3 presents the regions of the substrate domain of an uncoated and coated tool.
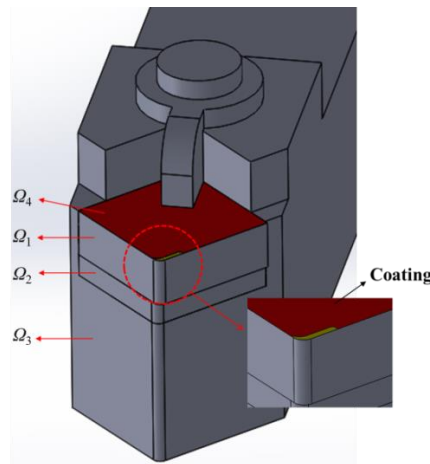

Figure 2. All the domains of the model and the coating detail.

Region S_1, highlighted in yellow, represents the contact area between the cutting tool and the workpiece, where the heat flux is applied during the cutting process. Region S_2 represents the entire cutting tool surface which is in contact with air, whose boundary conditions are natural convection and radiation. Region S_3 is the contact interface between the cutting tool and the tool holder. The model of the coated cutting tool (Fig. 3) is composed of the carbide substrate domain (Ω_1) and the coating domain (Ω_4). The regions on the coated cutting tool are the same as the uncoated cutting tool, except for S_4 which represents the upper part of the coating. Region S_1 is the same for the coated and uncoated tool model. This region was measured by Carvalho et al. [8] using an image system program with a video camera. A comparison of the numerical contact area of this work and the work of Carvalho et al. [8] is presented in Fig. 4.
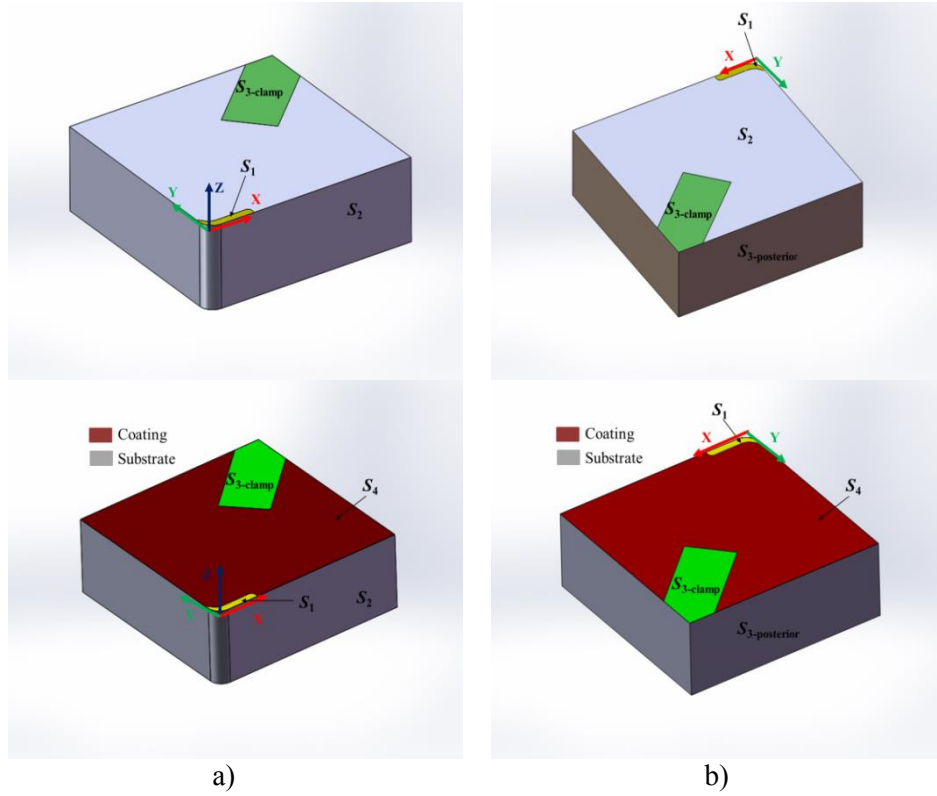
Figure 3. Domain of the coated and uncoated cutting tool: a) Contact interface with the workpiece, convection and radiation; b) Contact interface with the tool holder.
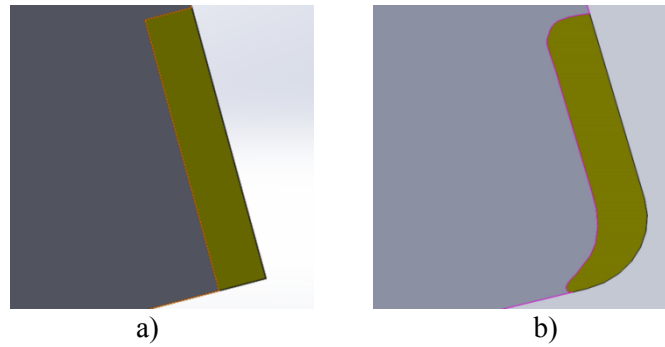
Figure 4. Comparison of the numerical area on the computational model: a) work of Carvalho *et.al* [8] and b) this work.

The tool holder domain (Ω_3) is also divided into two regions, once it receives part of the thermal energy from the cutting tool during the turning process. Region S_5 includes all the surfaces of the tool holder which are in contact with the shim and the cutting tool. The other surfaces comprehend the Region S_6, submitted to the boundary conditions of natural convection and radiation. The thermal contact between the carbide tool, shim and tool holder was considered perfect. Figure 5 shows the regions of the tool holder.
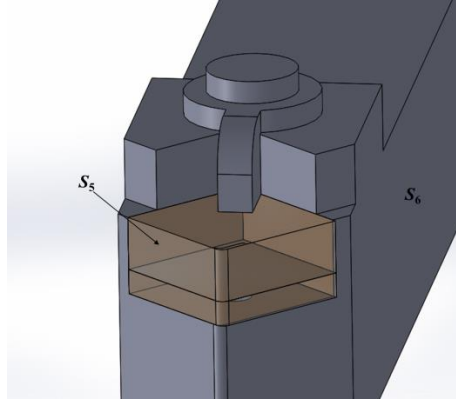
Figure 5. Tool holder domain with the contact interfaces and the surfaces subjected to natural convection and radiation conditions.

The thermal properties such as the thermal conductivity and thermal diffusivity of the carbide, coating materials and the AISI 1045 steel were taken from Grzesik *et al*. [13] using fitting data points. The emissivity curve of the carbide was obtained from Jiang *et al*. [14], whereas the emissivity for the coating materials and AISI 1045 steel was obtained from Yuste *et al*. [15], Wang et al. [16] and Polozine and Schaeffer [17], respectively.

2.2. Direct thermal model

The thermal model may be described by the non-linear transient three-dimensional diffusion equation:

$$\frac{\partial}{\partial x}\left(k(T)\frac{\partial T}{\partial x}\right)+\frac{\partial}{\partial y}\left(k(T)\frac{\partial T}{\partial y}\right)+\frac{\partial}{\partial z}\left(k(T)\frac{\partial T}{\partial z}\right)=\rho c(T)\frac{\partial T}{\partial t} \tag{1}$$

where x, y, and z are the Cartesian Coordinates, t the physical time, T the temperature, c the specific heat and ρ the density.

Subject to the following boundary conditions of convection and radiation

$$-k(T)\frac{\partial T}{\partial \eta}(x,y,z,t)=h(T)(T-T_{\infty})+\sigma\varepsilon(T)\left(T^{4}-T_{\infty}^{4}\right) \tag{2}$$

where k is the thermal conductivity, η the normal direction, h the heat transfer coefficient by convection, σ the Stefan-Boltzmann constant, ε the emissivity, and T_{∞} the room temperature.

In the contact area, the boundary condition of the imposed heat flux, q" is applied:

$$-k(T)\frac{\partial T}{\partial z}(x,y,0,t)=q" \tag{3}$$

The initial condition of the prescribed temperature is used for the entire domain as:

$$T(x,y,z,0)=T_{\infty} \tag{4}$$

The solution of the previous equations is obtained with the use of the finite element method, through the commercial software COMSOL *Multiphysics* 5.2. Due to the temperature gradients in the air and the gravitational field, there is an induction of natural convection currents around the assembly. In order to model the natural convection coefficient, which depends on the temperature, the software uses the empirical correlations from Incropera *et al*. [18].

2.3. Inverse thermal model

The inverse technique adopted in this work is the Specification Function. In this technique, a determined value of future time steps *r* is used to estimate the heat flux at the present instant [19]. In the resolution of the inverse problem, the Specification Function searches for a heat flux value that minimizes the objective function given in Eq. (5), for each time step. A MATLAB program with the software COMSOL *Multiphysics* 5.2 was used to estimate the heat flux.

$$F = \sum_{i=1}^{nt} \sum_{j=1}^{ns} \left(Y_{ij} - T_{ij} \right)^2 \tag{5}$$

where *F* is the objective function, *i* is the index to measure time, *nt* represents the total time of temperature measurements, *j* is the counter for the number of sensors and *ns* represents the number of temperature sensors.

3. Experimental procedure

One of the major problems in the thermal analysis of a turning process is accurately knowing the heat flux at the tool-chip interface. This work uses the experimental temperature data obtained by Carvalho *et al.* [8] to estimate the heat flux. The machining test was carried out in a conventional lathe IMOR MAXI-II-520-6CV without coolant. The material used in the experimental test was a cylindrical gray cast iron bar FC 20 EB 126 ABNT of 77 mm in external diameter. The insert and tool holder used were cemented ISO SNUN12040408 K20/Brassinter and ISO CSBNR 20K12/SANDVIK COROMAT, respectively. The temperatures were measured on accessible locations of the insert, the shim and the tool holder by using type K thermocouples (30 AWG) linked to a data acquisition system HP 75000 Series B controlled by a PC (Fig. 6). The location of the thermocouples used in the simulations and the cutting conditions to obtain the temperature data was according to the Brito *et al.* [4] work.
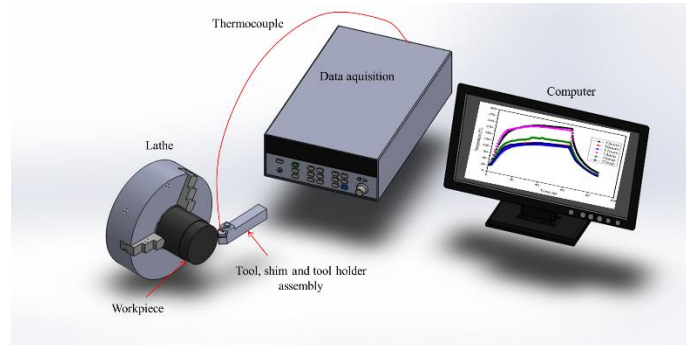
**Figure 6**. Experimental apparatus used to acquire the temperature signals in the tool during turning.

One of the improvements of this work is how the contact interface area is modelled. This numerical contact area had a shape closer to the real contact area (Fig. 5), while the numerical area used by Carvalho *et al.* [8] had a rectangular shape. The cutting conditions used to obtain the temperature data is shown in Tab. 2.

4. Results analysis

4.1. Heat flux

Once the experimental temperature values are known, the heat flux in the contact area can be calculated by minimizing the objective function (Eq. 5). Figure 7 presents the results of the heat flux obtained in this work and also compares with the heat flux results of Brito *et al.* [4]. Despite the fact of being the same physical problem, there are some differences among the heat flux values for each

work. Brito *et al*. [4] made some geometric simplifications, like using a solid shim instead of an L shape shim. Therefore, the authors did not take into account the variation of the heat transfer coefficient of convection and radiation in the numerical model. When this non-linearity is accounted, a higher estimated heat flux is expected due to a higher heat loss by convection and radiation.
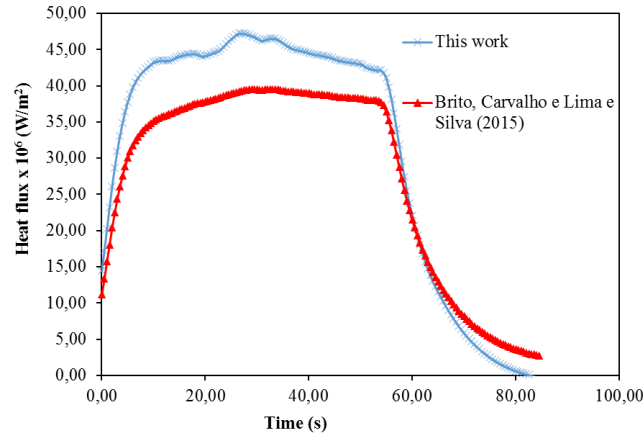

Figure 7. A Comparison between the estimated heat flux for this work and Brito et al. [4]**.**

4.2. Uncoated carbide tool

The temperature profile can be achieved by knowing the heat flux value in the contact area between the workpiece and the cutting tool. The first simulation was carried out considering an uncoated carbide tool. A numerical probe was placed in the contact area (Fig. 5) in order to obtain the temperature in this region. Through the software, the maximum, the average and the minimum temperature values can be calculated (Fig. 8). High variations of the temperature values can be observed in this figure, even with the small value of the contact area (1.43 mm^2). The maximum temperature reached was around 1097°C, the average temperature reached was around 963°C and the minimum temperature was also around 626°C. Figure 9 shows the isothermal temperature lines in the region near the contact area at instant $t = 28$ s.
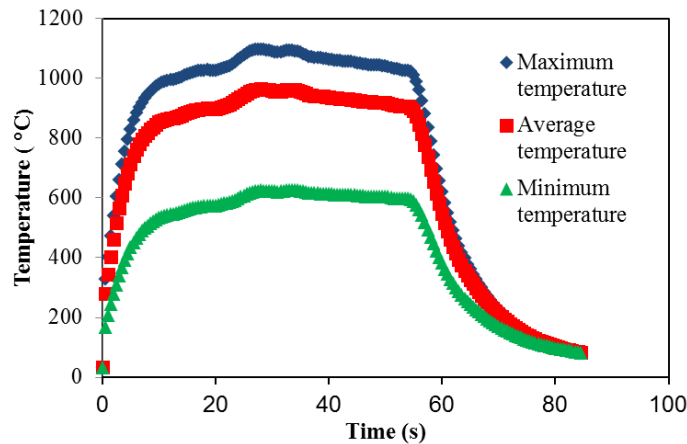

Figure 8. Maximum, average and minimum temperature in the contact area.
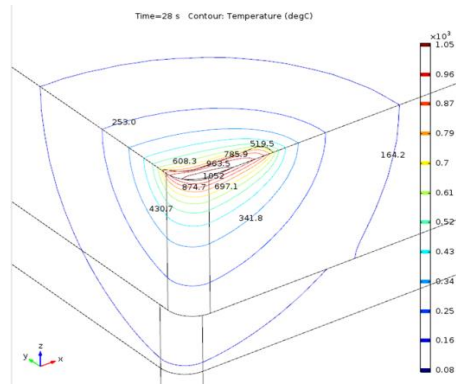
**Figure 9.** Isothermal temperature lines in the region near the contact area.

4.3. Coated carbide tools

The simulation described in Section 4.1 is repeated, but now considering the coating which is represented by a thin 10 μm thick layer. Figure 10 presents the isothermal temperature lines in the region near the contact area on the coated tool of TiN and Al_2O_3 at instant $t = 28$ s.

a)   b)
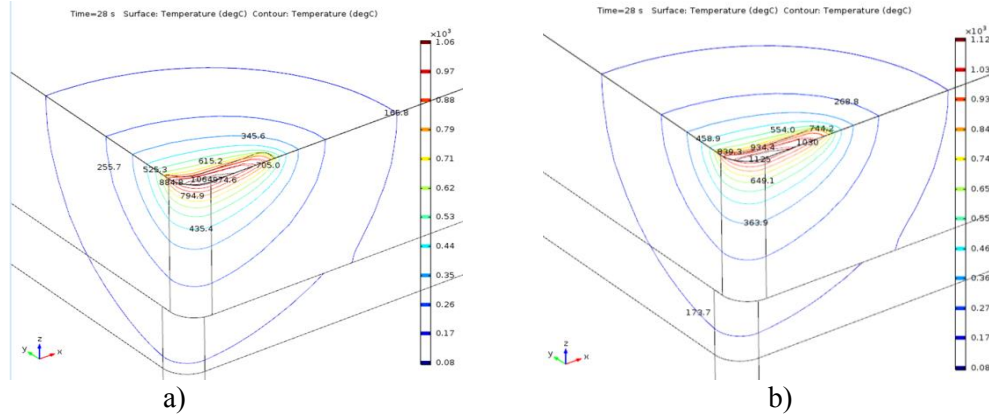
Figure 10. Isothermal temperature lines in the region near the contact area: a) TiN and b) Al_2O_3.

By analysing Figures 9 and 10, it can be noticed that the temperature in region of the contact area is higher on the coated tool than the uncoated tool. In order to better understand these results, Fig. 11a presents the maximum temperature in this region at instant $t = 28$ s, on the uncoated tool, TiN coated tool and the Al_2O_3 coated tool. Figure 11b shows the temperature differences between the coated tools and the uncoated tool.

a)   b)
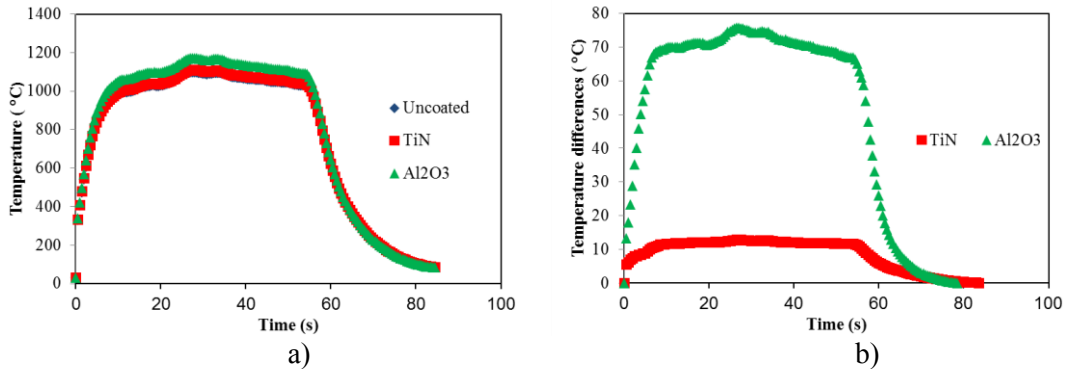
Figure 11. a) Maximum temperature in the coated area for the uncoated and coated tools and b) temperature differences between the coated tools and the uncoated tool.

It can be verified in Fig. 11a that the curves of maximum temperature of the coated and uncoated tools have the same behaviour. The maximum temperature curve of the TiN coated tool overlaps the maximum temperature curve of the uncoated tool, not presenting a relevant temperature difference. This fact can be noticed in Fig. 11b at instant $t = 28$ s. The maximum temperature difference between the TiN coated tool and the uncoated tool is around 12.7° C. For the Al_2O_3 coated tool the maximum temperature curve is above the maximum temperature curve of the uncoated tool, as can be seen in Fig. 11a. In Figure 11b, at instant $t = 28$ s, the maximum difference of temperature between the Al_2O_3 coated tool and the uncoated tool is around 75.5 °C. In the work of Brito *et al.* [7], the maximum temperature difference obtained was around 8.2 °C using the same 10 μm thick coated carbide tool.

Observing the previous figures it can be concluded the coating retains the heat on the top face of the cutting tool, not letting the heat penetrate the cutting tool substrate and thus increasing the cutting tool lifespan. The Al_2O_3 coating presents a better insulating characteristic than the TiN since it has a lower thermal conductivity value.

4.4. Coating thickness influence

As previously shown, the coatings used in the cutting tools have insulating characteristics and play the role of protecting the substrate of the cutting tool with respect to heat. To further evidence this effect, the simulations of Section 4.3 are repeated considering thicker coatings: 20 μm, 50 μm and 100 μm (Tab. 1 and Fig. 12).

Table 1. Differences of the maximum temperature in the contact area between the coated and uncoated tool for different thickness coating values.

Coating thickness (μm)	TiN	Al_2O_3
10	12.7 °C	75.5 °C
20	25.2 °C	151.5 °C
50	61.1 °C	351.8 °C
100	117,1 °C	663.5 °C
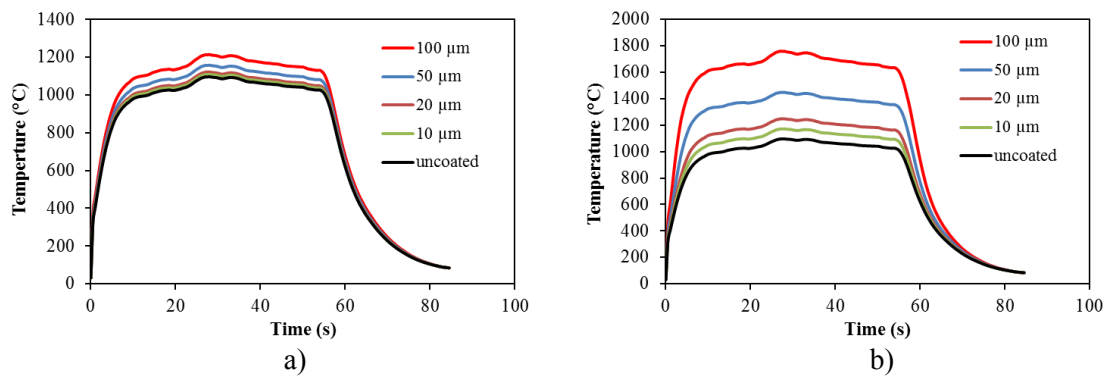
Figure 12. Maximum temperature curve in the contact area for different coating thickness values: a) TiN and b) Al_2O_3.

When the coating thickness value of both materials is increased, the maximum temperature in the contact area also increases (Fig. 12). Table 1 also shows this fact where the maximum temperature difference in the contact area between the coated tools and the uncoated tool for different coating thickness values can be seen. Figure 13 presents the temperature field in the region near to the contact interface area for the uncoated tool and the Al_2O_3 coated tool for different thickness coating at the instant of $t = 28$ s. This figure shows the heat behaviour when the thickness coating increases.
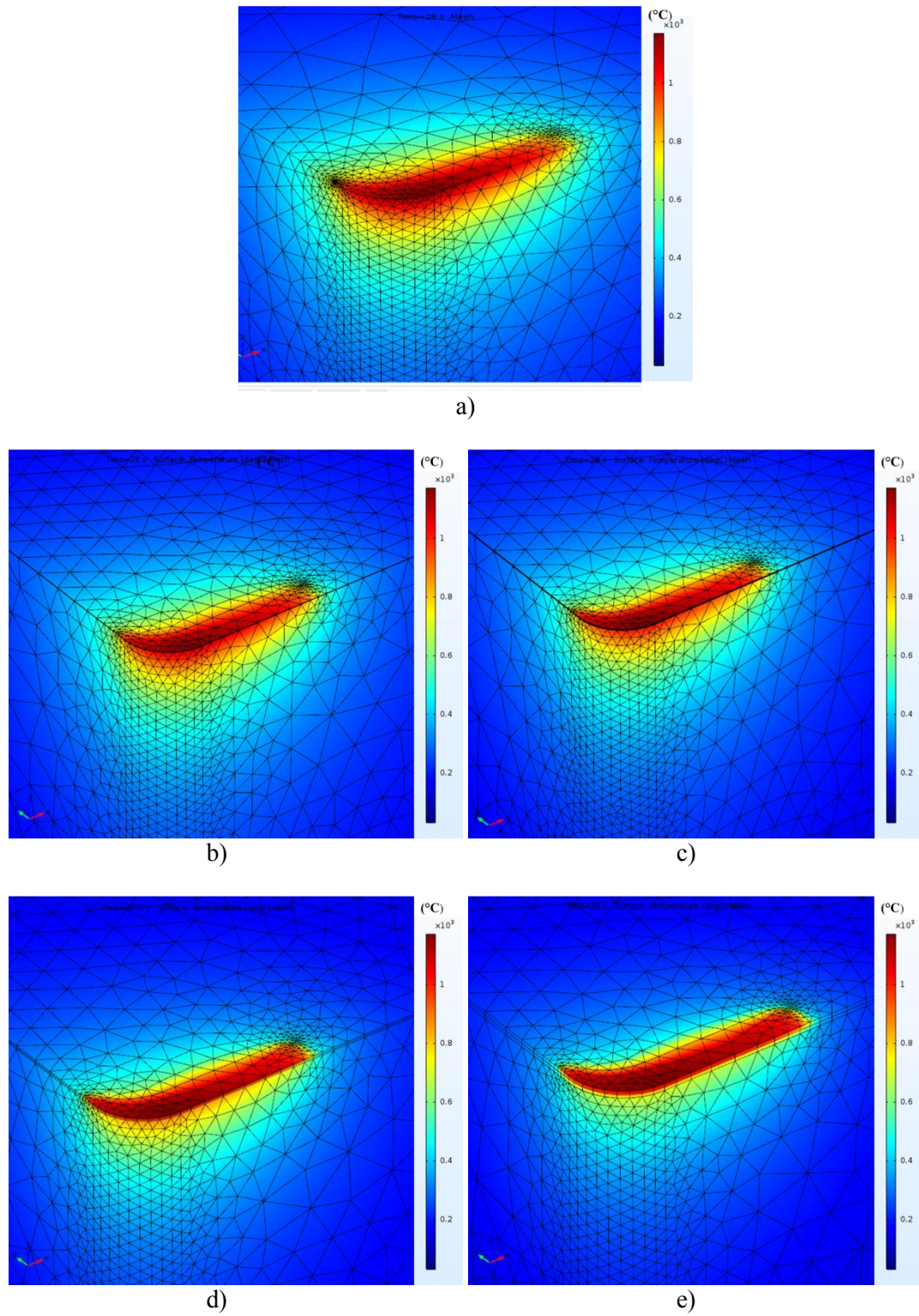
Figure 13. Influence of the Al$_2$O$_3$ coating thickness in the cutting tool temperature field: a) uncoated tool, b) 10µm, c) 20 µm, d) 50 µm and e) 100 µm.

In the Figure 13a, which represents the uncoated tool, can be noticed that the heat penetrates deeply the cutting tool substrate and consequently the temperature field is large. Inserting the coating in the cutting tool (Figure 13b) the temperature field begin decreasing slightly. Increasing the coating thickness (Fig.13c to Fig.13e) the temperature field decreases even more. It can be noticed by the red color in the figures. Thus, the coating holds the heat on the upper face of the cutting tool and did not let it goes to the cutting tool substrate which would be harmful for the cutting tool lifespan.

5. Conclusions

This work presented the coating effect on the temperature field of the cemented carbide cutting tool. The coating effect was observed by comparing the peak temperature between the uncoated and coated material. The coating thickness was numerical increased to highlight the coat influence on the cemented carbide cutting tool. Although the small contact area, the coated and uncoated carbide cutting tool presented a peak difference in the cutting region of 12.7 °C for the TiN and 75.5 °C for the Al_2O_3. The 10-µm-thick coated tool models presented the expected behavior, once the maximum temperature in the contact area was higher when compared to the maximum temperature in the contact area of the uncoated tool. By increasing the coating thickness, the maximum temperature in the contact area also increases. The best results were obtained using the Al_2O_3 coating, once it has a thermal conductivity value lower than the thermal conductivity value of the TiN coating. Thus, the coating fulfils its role of protecting the substrate of the cutting tool with respect to heat.

References

[1]   Deppermann M and Kneer R 2015 Determination of the heat flux to the workpiece during dry turning by inverse methods *Prod. Eng.* **9** 465–71

[2]   Lazard M and Remy B 2008 HEAT FLUX AND TEMPERATURE ESTIMATION DURING CUTTING PROCESS THROUGH REGULARIZATION TECHNIQUE *5th European Thermal-Sciences Conference* vol 1(The Netherlands)

[3]   Liang L, Xu H and Ke Z 2013 An improved three-dimensional inverse heat conduction procedure to determine the tool-chip interface temperature in dry turning *Int. J. Therm. Sci.* **64** 152–61

[4]   Brito R F, Carvalho S R and Lima E Silva S M M 2015 Experimental investigation of thermal aspects in a cutting tool using comsol and inverse problem *Appl. Therm. Eng.* **86** 60–8

[5]   De Carvalho S R, Dos Santos M R, De Souza P F B, Guimarães G and De Lima E Silva S M M 2009 Comparison of inverse methods in the determination of heat flux and temperature in cutting tool during a machining process *High Temp. - High Press.* **38** 5–9

[6]   Liang L and Quan Y 2013 Investigation of heat partition in dry turning assisted by heat pipe cooling *Int. J. Adv. Manuf. Technol.* **66** 1931–41

[7]   Brito R F, Carvalho S R de, Lima e Silva S M M de and Ferreira J R 2009 Thermal analysis in coated cutting tools *Int. Commun. Heat Mass Transf.* **36** 314–21

[8]   Carvalho S R, Lima S M M, Machado A R and Guimar G 2006 Temperature determination at the chip – tool interface using an inverse thermal model considering the tool and tool holder *J. Mater. Process. Technol.* **179** 97–104

[9]   Shabgard M and Akhbari S 2016 An inverse heat conduction method to determine the energy transferred to the workpiece in EDM process *Int. J. Adv. Manuf. Technol.* **83** 1037–45

[10]   Gerlich V, Sulovská K and Zálešák M 2013 COMSOL Multiphysics validation as simulation software for heat transfer calculation in buildings: Building simulation software validation *Meas. J. Int. Meas. Confed.* **46** 2003–12

[11] Greiby I, Mishra D K and Dolan K D 2014 Inverse method to sequentially estimate temperature-dependent thermal conductivity of cherry pomace during nonisothermal heating *J. Food Eng.* **127** 16–23

[12] Suarez V, Hernández Wong J, Nogal U, Calderón A, Rojas-Trigos J B, Juárez A G and Marín E 2014 Study of the heat transfer in solids using infrared photothermal radiometry and simulation by COMSOL Multiphysics *Appl. Radiat. Isot.* **83** 260–3

[13] Grzesik W, Niesłony P and Bartoszuk M 2009 Modelling of the Cutting Process Analytical and Simulation Methods *Adv. Manuf. Sci. Technol.* **33** 5–29

[14] Jiang F, Zhang T and Yan L 2016 Estimation of temperature-dependent heat transfer coefficients in near-dry cutting *Int. J. Adv. Manuf. Technol.* **86** 1207–18

[15] Yuste M, Galindo R E, Sánchez O, Cano D, Casasola R and Albella J M 2010 Correlation between structure and optical properties in low emissivity coatings for solar thermal collectors *Thin Solid Films* **518** 5720–3

[16] Wang Y M, Tian H, Shen X E, Wen L, Ouyang J H, Zhou Y, Jia D C and Guo L X 2013 An elevated temperature infrared emissivity ceramic coating formed on 2024 aluminium alloy by microarc oxidation *Ceram. Int.* **39** 2869–75

[17] Polozine A and Schaeffer L 2005 Exact and approximate methods for determining the thermal parameters of the forging process *J. Mater. Process. Technol.* **170** 611–5

[18] Bergman T L, Lavine A S, Incropera F P and Dewitt D P 2011 *Fundamentals of Heat and Mass Transfer* (Hoboken, NJ: John Wiley & Sons)

[19] Beck V J, Blackwell B and Clair C A ST. 1985 *Inverse Heat Conduction: Ill-Posed Problems,* (Wiley)